Journal of Materials Chemistry B

ROYAL SOCIETY OF CHEMISTRY

PAPER

View Article Online
View Journal | View Issue

Cite this: J. Mater. Chem. B, 2025, 13, 10300

A novel biomaterial derived from the skin secretion of *Andrias davidianus* for dentinal tubule occlusion†

Yongxiang Zeng,[abcd] Lin Yang,[abcd] Na Wu,[abcd] Hong Chen,[abcd] Ximu Zhang*[abcd] and Deqin Yang *[abcdef]

Dentin hypersensitivity is a common challenge for dentists and patients. Occluding dentinal tubules through dentin remineralization is considered an alternative therapeutic approach to manage dentin hypersensitivity. The skin secretion of *Andrias davidianus* (SSAD) contains various binding functional groups. In this study, SSAD hydrolysate was prepared with tris(2-carboxyethyl)phosphine reduction. Its binding ability to acid-etched dentin, as well as its efficacy in dentin remineralization and tubule occlusion were evaluated. The results demonstrated that SSAD hydrolysate could easily and firmly bind to the surface of collagen fibrils. This hydrolysate could stabilize calcium and phosphorus ions in an amorphous state and induce the accumulation of apatite on the dentin surface. After 4 weeks of incubation in artificial saliva, dentinal tubules treated with 0.5 mg mL^{-1} SSAD hydrolysate were evidently sealed by regenerated minerals. The deposited minerals were observed deep within the dentinal tubules (up to 30 ± 5 μm). X-Ray diffraction and energy-dispersive X-ray analyses further confirmed that the regenerated minerals were mainly hydroxyapatite. Sequentially, stable occlusion after acid challenge and significant reduction in dentin permeability were achieved. The microhardness value of the remineralized dentin treated with SSAD hydrolysate was significantly increased. In addition, the proliferation, migration, mineralization, and odontogenic differentiation of human dental pulp stem cells were promoted. Animal experiments indicated that SSAD hydrolysate could also occlude dentinal tubules in the oral environment. In conclusion, our work provides an experimental basis for the potential use of SSAD hydrolysate for treating dentin hypersensitivity.

Received 9th April 2025,
Accepted 16th July 2025

DOI: 10.1039/d5tb00823a

rsc.li/materials-b

1. Introduction

Dentin hypersensitivity, a prevalent and recurrent dental complaint, presents with short and sharp pain.[1,2] This dental condition is common among patients with dentin exposure caused by caries, attrition, wedge-shaped defects, gingival recession, and trauma.[3,4] According to the hydrodynamic hypothesis, occluding dentinal tubules to reduce fluid movement and subsequent impulse transmission represents an effective method for alleviating relevant clinical symptoms.[5] Although several therapeutic approaches, such as toothpaste or mouth rinses with desensitizing agents, laser irradiation, and filling repair, have been used to occlude dentinal tubules, their long-term effectiveness remains unsatisfactory.[6–9] Recently, occlusion agents capable of inducing biomimetic mineralization have been proposed to repair mineral-depleted dentin and subsequently occlude dentinal tubules.[10–12] The role of non-collagenous proteins (NCPs) in dentin remineralization has been widely discussed.[13] Some researchers believe that NCPs can initiate apatite nucleation and control the growth of hydroxyapatite (HA) crystals.[14] However, obtaining intact NCPs is difficult and economically unfeasible.[15] Therefore, strategies involving the coating of biomimetic NCP analogs onto the demineralized dentin surface have been adopted to facilitate dentin remineralization.

Li *et al.*[16] successfully synthesized the amyloid-like protein lysozyme coupled with polyethylene glycol (lyso-PEG), which is

[a] The Affiliated Stomatological Hospital of Chongqing Medical University, Chongqing, 404100, P. R. China. E-mail: zhangximu@hospital.cqmu.edu.cn, yangdeqin@hospital.cqmu.edu.cn
[b] Chongqing Key Laboratory of Oral Diseases, Chongqing 404100, P. R. China
[c] Chongqing Municipal Key Laboratory of Oral Biomedical Engineering of Higher Education, Chongqing 404100, P. R. China
[d] Chongqing Municipal Health Commission Key Laboratory of Oral Biomedical Engineering, Chongqing 404100, P. R. China
[e] Department of Conservative Dentistry and Endodontics, Shanghai Stomatological Hospital & School of Stomatology, Fudan University, Shanghai, 200433, P. R. China
[f] Shanghai Key Laboratory of Craniomaxillofacial Development and Diseases, Fudan University, Shanghai, 200433, P. R. China

† Electronic supplementary information (ESI) available. See DOI: https://doi.org/10.1039/d5tb00823a

rich in β-sheets and can penetrate narrow and deep dentinal tubules. The lyso-PEG oligomers further achieved deep and steady occlusion of dentinal tubules.[16] Han *et al.*[17] extracted multifunctional polyphenol ingredients from gallnut. Their experiments suggested that the hydroxyl functional groups in phenols could accumulate calcium and phosphate, which is of great significance for the repair of dental hard tissues and the occlusion of dentinal tubules. Saravana Karthikeyan *et al.*[18] demonstrated that eggshell-derived nanohydroxyapatite combined with carboxymethyl chitosan enhanced dentin remineralization by mimicking NCP-mediated mineralization pathways, leading to complete tubular occlusion and improved microhardness. Similarly, Rani *et al.*[19] reported that the combination of eggshell nanohydroxyapatite and phytosphingosine promotes mineral deposition and stabilizes collagen fibrils in demineralized dentin. In summary, these studies highlight the significant potential of various biomaterials and peptides to mimic NCPs to enhance dentin remineralization and protect dental structures, representing promising solutions for addressing dentin hypersensitivity and promoting overall oral health.

Our previous research on the skin secretion of *Andrias davidianus* (SSAD) demonstrated that the SSAD hydrogel has strong tissue adhesion properties and exhibits excellent biocompatibility, promoting soft tissue repair and enhancing wound healing.[20] SSAD is a complex mixture rich in proteins, amino acids, antimicrobial peptides, and mucopolysaccharides.[21] These proteins contain tyrosine, phenylalanine, and tryptophan, which possess functional groups such as phenolic hydroxyl groups, amino groups, and benzene rings, all of which are believed to facilitate bonding effects.[21–25] Based on the excellent adhesion ability of SSAD, we hypothesized that it could represent an excellent candidate for the surface modification of the dentin matrix, effectively binding to exposed collagen fibrils. After reducing the disulfide bonds of SSAD proteins with tris(2-carboxyethyl)phosphine (TCEP), we obtained SSAD hydrolysate with abundant biochemically active end-groups, which may be able to perform the function of NCPs and induce dentin mineralization. Moreover, Zhang *et al.*[26] applied TCEP-reduced functional SSAD hydrolysate to bone defects and observed osteogenic-associated stem cell recruitment and the formation of multiple bone centers. Component analysis has also revealed that SSAD contains various growth factors that stimulate tissue repair.[26] As a desensitizing material applied to dentin, it is crucial for SSAD to exhibit good biocompatibility. Therefore, the investigation of its biological performance is of great significance.

In this study, SSAD hydrolysate was prepared and coated onto acid-etched dentin (Scheme 1). We hypothesized that SSAD hydrolysate could effectively bind to collagen fibrils, induce dentin remineralization, and subsequently occlude dentinal tubules. Experiments with human dental pulp stem cells (HDPSCs) were conducted to evaluate the biocompatibility of SSAD hydrolysate, while animal experiments were performed to simulate the dentin remineralization effects of SSAD hydrolysate in the oral environment.

2. Materials and methods

2.1. Preparation and characterization of SSAD hydrolysate

The SSAD powder was prepared according to our previous protocol.[20,27,28] Briefly, healthy male *Andrias davidianus* (Chinese Giant Salamanders) (3–5 years old, 65–110 cm in length, and 2.8 ± 0.7 kg in weight) from a Chinese Giant Salamander Breeding Base in Chongqing, China, was cleaned with fresh water. Chinese giant salamanders have abundant mucous glands on their dorsal skin. Gentle scraping of the dorsal skin with a stainless steel curette induced mucus secretion. As a non-invasive procedure, this does not cause pain to the giant salamanders. Each adult animal typically yielded more than

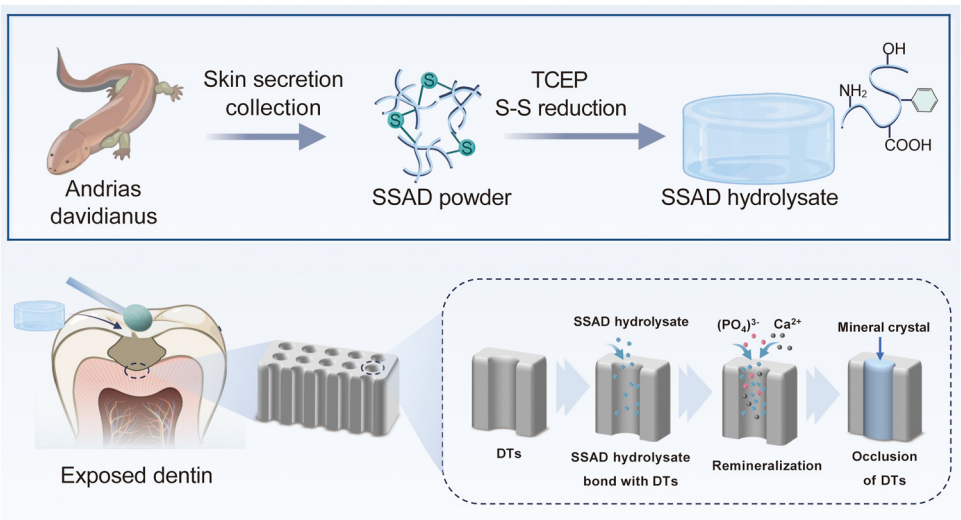

Scheme 1 Schematic illustration of the preparation of skin secretion of *Andrias davidianus* (SSAD) hydrolysate. Remineralization of dentin and the occlusion of dentinal tubules (DTs) induced by SSAD hydrolysate.

20 mL of mucus during harvesting. All experiments were conducted in strict accordance with China's Animal Protection Law, and no Chinese giant salamanders were sacrificed. The skin secretions were washed with phosphate buffer saline (PBS), freeze-dried, and ground into 300-mesh powder. Subsequently, a 4 mg mL^{-1} TCEP solution was prepared, and 200 mg of SSAD powder was added to 10 mL of the TCEP solution at 4 °C for 24 h. After centrifugation and 48 h of dialysis, SSAD hydrolysate was obtained, and its concentration was measured using a Bradford protein assay kit.

The secondary structures of SSAD before and after TCEP reduction were characterized using circular dichroism (CD) spectroscopy. The measurements were conducted from 180 to 260 nm at a rate of 200 nm min^{-1}. After eight scans, the average data were obtained. HDPSCs were used to evaluate the cytotoxicity of SSAD hydrolysate. The details of HDPSCs isolation, culture, and identification are presented in the ESI† (Fig. S1). The cell density was adjusted to 5000 cells per well of a 96-well plate. The cells were then cultured with SSAD hydrolysate at different protein concentrations (0.05, 0.1, 0.5, 1, and 2 mg mL^{-1}) for 24 h. Cell viability was analyzed using cell counting kit-8 (CCK-8). Cells cultured in PBS were used as the control group. As per the kit instructions, 10% (v/v) CCK-8 solution was added and incubated in the dark for 1 h, before recording optical density at 450 nm. Each experiment was repeated three times.

2.2. Effects of different SSAD hydrolysate concentrations on dentin remineralization

2.2.1. Preparation of dentin specimens. Human exfoliated third molars free of caries, defects, cracks, or abrasions were collected after receiving informed consent from patients. The experiment was approved by the Ethics Committee of Chongqing Medical University (CQHS-REC-2020; LS No. 68). After scraping off the extra soft tissue and washing with PBS, the molars were immersed in 0.1% (w/v) thymol solution at 4 °C for subsequent application. The teeth were sliced perpendicular to the long axis below the enamel–dentinal junction using a hard tissue saw (EXAKT, Germany) with cooling water. Next, 130 dentin disks, each with a thickness of 1 mm, were prepared for subsequent experiments. The dentin disks were polished with silicon carbide sandpapers (600–2000 mesh) and then cleaned in deionized water with ultrasonication (400 W) for 15 min. To prepare the dentin hypersensitivity model, dentin tablets were soaked in 0.5 M ethylenediaminetetraacetic acid (EDTA, pH 8.0) for 30 min and then ultrasonicated in deionized water (400 W) for 15 min.[29]

2.2.2. Bonding capability of SSAD hydrolysate on dentin. The EDTA acid-etched dentin slices were gently blown dry and then coated with different concentrations of SSAD hydrolysate (0.05, 0.1, 0.5, 1, and 2 mg mL^{-1}) using a small brush for 20 s. The coated dentin samples were then subjected to ultrasonic treatment (400 W) for 1 min. Field-emission scanning electron microscopy (FESEM) (ZEISS Gemini 300, Germany) was used to observe the bonding stability of SSAD hydrolysate on the dentin surface before and after ultrasonic treatment.

2.2.3. Contact angle measurement. Acid-etched dentin surfaces were coated with SSAD hydrolysate of different concentrations (0.05, 0.1, 0.5, 1, and 2 mg mL^{-1}) or with deionized water as a control and then dried at room temperature. Using a micro-syringe, 5 μL of deionized water was slowly dropped onto the surface of the pre-coated dentin. After 15 s, the static contact angles were documented with a contact-angle measuring instrument (Beijing Global Hengda, China). Each group was measured five times (n = 5).

2.2.4. Remineralization capability of SSAD hydrolysate on dentin. To investigate the effects of SSAD hydrolysate on dentin remineralization, the hydrolysate was applied to the acid-etched dentin at concentrations of 0.05, 0.1, 0.5, 1, and 2 mg mL^{-1}, before incubating in artificial saliva (AS) (pH 7.02) at 37 °C for 1 week. The AS, containing $CaCl_2$ (1.5 mM), KH_2PO_4 (0.9 mM), KCl (130 mM), NaN_3 (1.0 mM), and 4-(2-hydroxyethyl)-1-piperazineethanesulfonic acid (HEPES) (20 mM), was prepared as previously reported and refreshed every 24 h.[30] The dentin morphology was detected using FESEM.

2.3. Remineralization of reconstituted collagen

Single-layer reconstituted collagen was used to observe the effects of SSAD hydrolysate on dentin remineralization. Briefly, a 0.05 mg mL^{-1} type I rat tail collagen solution was dripped onto 300-mesh Ni transmission electron microscopy (TEM) grids. Collagen fibrils were self-assembled with 1% ammonia vapor and then maintained at 37 °C for 12 h. Glutaraldehyde (0.05 wt%) was used to cross-link the collagen fibrils for 1 h. SSAD hydrolysate (0.5 mg mL^{-1}) or deionized water (as the control) was dripped on the TEM grids covered with collagen fibrils and air-dried. The samples were then floated over AS at 37 °C for a designated time (6, 12, and 24 h). The grids were retrieved for TEM (HT7700, Hitachi, Japan) observation after washing in deionized water and air drying.

2.4. Assessment of dentinal tubule occlusion

2.4.1. FESEM morphology of dentin. Based on the above results, we found that the 0.5 mg mL^{-1} SSAD hydrolysate group had better dentin remineralization efficacy than the other groups. To further evaluate its tubule-sealing efficacy, acid-etched dentin disks treated with 0.5 mg mL^{-1} SSAD hydrolysate or deionized water (as the control) were incubated in AS at 37 °C for 1, 2, and 4 weeks, and the solution was replaced daily. FESEM and energy-dispersive X-ray (EDX) were used for morphology observation and element composition detection of dentin.

2.4.2. X-ray diffraction analysis. X-ray diffraction (XRD; Bruker D8 advance, Germany) patterns were applied on dentin disks before and after remineralization for 4 weeks to examine the type of biomineralized crystal and the orientation degree of crystallinity. Untreated dentin and EDTA-etched dentin were also analyzed for comparison.

2.4.3. Acid resistance. After 4 weeks of remineralization, dentin specimens were subjected to a 6% citric acid challenge for 1 min. After rinsing with deionized water, the surface and cross-section morphology were observed using FESEM.

2.4.4. Permeability measurement. The permeability of dentin slices after EDTA acid etching, remineralization for 4 weeks, and citric acid challenge (n = 6) was measured. A modified hydraulic conductance system was constructed with a water reservoir (20 cm) to simulate pulpal pressure, as previously reported.[31] This system allowed for the measurement of dentin permeability. Hollow rubber rings with an inner diameter of 7 mm were placed on the top and bottom of the dentin slices and were then fixed between the resin fixtures. An air bubble was injected into the 25-μL capillary tube through a syringe, and the distance that the air bubble moved within 5 min was recorded to calculate the flow rate (μL min^{-1}). Then, the flow rate was divided by the measurable area of the dentin slice (cm^2) and the water pressure (cmH_2O) to obtain the water conductivity (Lp). The water conductivity of the EDTA-etched dentin slices was considered the maximum dentin permeability (Lp = 100%). For each sample, the dentin permeability was documented as a proportion (Lp%) relative to the permeability of EDTA-etched dentin, and the measurement process was repeated three times.

2.4.5. Assessment of dentin microhardness. The Vickers hardness test (HVS-10Z, Jingbo Company, China) was conducted to measure the microhardnesses of intact dentin, acid-etched dentin, and remineralized dentin in the SSAD hydrolysate and control groups.[18,19,32] The loading force was 50 g with a dwell time of 10 s. Five indentations were detected in each dentin sample.

2.4.6. Commercial sealants for dentinal tubule occlusion. The EDTA acid-etched dentin slices were gently blown dry, painted with Duraphat agent (Colgate-Palmolive, UK) using a small brush, and maintained at room temperature for 4 h until the coating hardened. The other dentin slices in the Gluma desensitizer group were air-dried, coated with Gluma desensitizer (Kulzer, Germany) for approximately 60 s, and gently blown until the liquid film disappeared. The treatment was repeated, and the dental surfaces were rinsed with water. The coated dentin samples were then subjected to ultrasonic treatment (400 W) for 1 min. FESEM was used to observe the morphology of the dentin surface before and after ultrasonic treatment.

2.5. Biocompatibility evaluation

HDPSCs were isolated, cultured, and identified, as presented in the ESI.† Cells at passages 3–5 were used to further evaluate the biocompatibility of 0.5 mg mL^{-1} SSAD hydrolysate.

2.5.1. Cell proliferation essays. The cell density was adjusted to 5000 cells per well of a 96-well plate. The cells were treated with 0.5 mg mL^{-1} SSAD hydrolysate or PBS as a control and cultured for 1, 3, and 5 days. CCK-8 was used to evaluate the effect of SSAD hydrolysate on cell proliferation. According to the kit instructions, 10% (v/v) CCK-8 solution was added and incubated in the dark for 1 h, before measuring the optical density at 450 nm. Each experiment was repeated three times.

2.5.2. Scratch wound-healing assay. A wound-healing assay was performed to assess the effects of SSAD hydrolysate on cell migration. HDPSCs were cultured in six-well plates with 5×10^5 cells per well. When the fusion degree of the cells reached 90%, a 200-μL pipette tip was used to make linear scratches with a uniform width. The floating cell fragments were then gently rinsed with a sterile PBS solution, and serum-free α-MEM medium with 0.5 mg mL^{-1} SSAD hydrolysate or PBS was added. An inverted phase-contrast microscope was used to record cell migration at 0 and 24 h. The relative healing area of the cells was calculated using ImageJ software.

2.5.3. Transwell migration assay. Briefly, the HDPSC density was adjusted to 3×10^5 cells per well and incubated in the upper chamber of a transwell with 100 μL of α-MEM, while 800 μL of α-MEM medium with 0.5 mg mL^{-1} SSAD hydrolysate or PBS was added to the lower chamber. Twenty-four hours after cell incubation, the upper chamber was removed and gently washed with PBS. Non-migrated cells on the upside were wiped off with cotton swabs. The migrated cells were fixed in 4% paraformaldehyde for 15 min and washed twice with PBS. The upper chambers were then soaked in 0.1% crystal violet (15 min) for cell staining and rinsed with PBS. Microscopic images were captured, and cell counts were performed to quantify the number of migrated cells.

2.5.4. Alkaline phosphatase (ALP) activity test. For the ALP activity test, the HDPSC density was adjusted to 2×10^5 cells per well and cultured with 0.5 mg mL^{-1} SSAD hydrolysate or PBS in odontogenic induction (OI) medium in six-well plates. The OI medium was prepared as described in the (ESI†).[33] After 14 days of incubation, ALP staining and the activity assay were performed. Cells were fixed in 4% paraformaldehyde for 15 min and washed twice with PBS. The BCIP/NBT ALP color development kit was used for staining (30 min in the dark). The morphological characteristics of the stained cells were captured using an inverted microscope. To assess ALP activity, cell lysis was performed in 1% Triton X-100 at a temperature of 4 °C. The BCA protein assay kit was used to quantify the total protein content. The ALP activity levels were measured using an ALP assay kit and were normalized relative to the total protein concentration. The absorbance was measured at 405 nm.

2.5.5. Alizarin red staining. Next, alizarin red staining was conducted to evaluate calcium nodule formation in HDPSCs. Briefly, cells (2×10^5 cells per well of a six-well plate) were cultured in OI medium with or without SSAD hydrolysate (0.5 mg mL^{-1}). After 14 days of incubation, the culture medium was removed, and the cells were fixed in 4% paraformaldehyde for 15 min, before washing twice with PBS. Staining was performed with 1% alizarin red S solution (pH 4.2) for 10 min. The stained cells were imaged using an inverted microscope. For quantification, 10% cetylpyridinium chloride was applied to extract the stain. The absorbance was measured at 620 nm.

2.5.6. Odontogenic-related gene expression. Next, quantitative reverse transcriptase-polymerase chain reaction (qRT-PCR) was performed to analyze the expression of odontogenic-related genes. HDPSCs (5×10^5 cells per well of a six-well plate) were cultured with or without SSAD hydrolysate (0.5 mg mL^{-1}). After 7 days of incubation, total RNA was extracted with TRIzol reagent. A NanoDrop2000 spectrophotometer (Thermo Scientific, Waltham, MA, USA) was used to test the purity (A260/A280) and

Table 1 qRT-PCR primers used for odontogenic differentiation

Gene	Primer sequence
GAPDH	Forward: GGAGTCCACTGGCGTCTTCA Reverse: GTCATGAGTCCTTCCACGATA
DSPP	Forward: GCTGGCCTGGATAATTCCGA Reverse: CTCCTGGCCCTTGCTGTTAT
DMP-1	Forward: GAGATAACCCCGACCCCACA Reverse: GAGAGTGTGTGCGAGCTGTC

concentration of RNA. Subsequently, complementary DNA (cDNA) was reverse transcribed using the Prime Script TM RT kit. qRT-PCR was performed using an Applied Biosystems ABI 7500 System (Bio-Rad Laboratories, Hercules, CA, USA). The relative mRNA expression levels of dentin sialophosphoprotein (*DSPP*) and dentin matrix protein-1 (*DMP-1*) were normalized to GAPDH, analyzed using the $2^{-\Delta\Delta Ct}$ method, and determined using cycle threshold (Ct) values. The primers used are listed in Table 1.

2.6. Animal experiments

Eight- to ten-week-old male Sprague–Dawley (SD) rats (200–250 g, five rats per group) were used for *in vivo* experiments.[16,32,34,35] The Animal Experimental Ethics Committee of the Chongqing Medical University approved the experiments. Dentin specimens with a uniform thickness of 1 mm were prepared and perforated for fixation in the oral cavity. The dentin slices were then acid-etched and treated with 0.5 mg mL^{-1} SSAD hydrolysate or deionized water. Stainless steel wire was passed through the holes to fix the dentin samples between the first molars and the upper central incisors. During the experiment, the rats were fed a soft diet to better protect the specimens from mechanical damage. All specimens were cultivated for 4 weeks, cleaned with deionized water, and then analyzed using FESEM and EDX.

2.7. Statistical analyses

The results are expressed as the mean ± standard deviation and were analyzed by one-way ANOVA or *t*-test using SPSS 21.0 (SPSS Software, USA). The Tukey method was used for *post hoc* tests. The statistical significance levels are represented as $*p < 0.05$, $**p < 0.01$, and $***p < 0.001$. Each experiment was performed three times.

3. Results

3.1. Characterization of SSAD hydrolysate

SSAD hydrolysate was prepared as shown in Fig. 1(A). When the SSAD powder (300-mesh) was mixed with TCEP solution, clumps of hydrogel were produced, which may have been induced by the hydration reaction.[20] After a 24-h reduction reaction with TCEP, the SSAD hydrogel was dissolved. The supernatant was collected by centrifugation, and a transparent SSAD hydrolysate was obtained after the dialysis process to remove the TCEP residue.

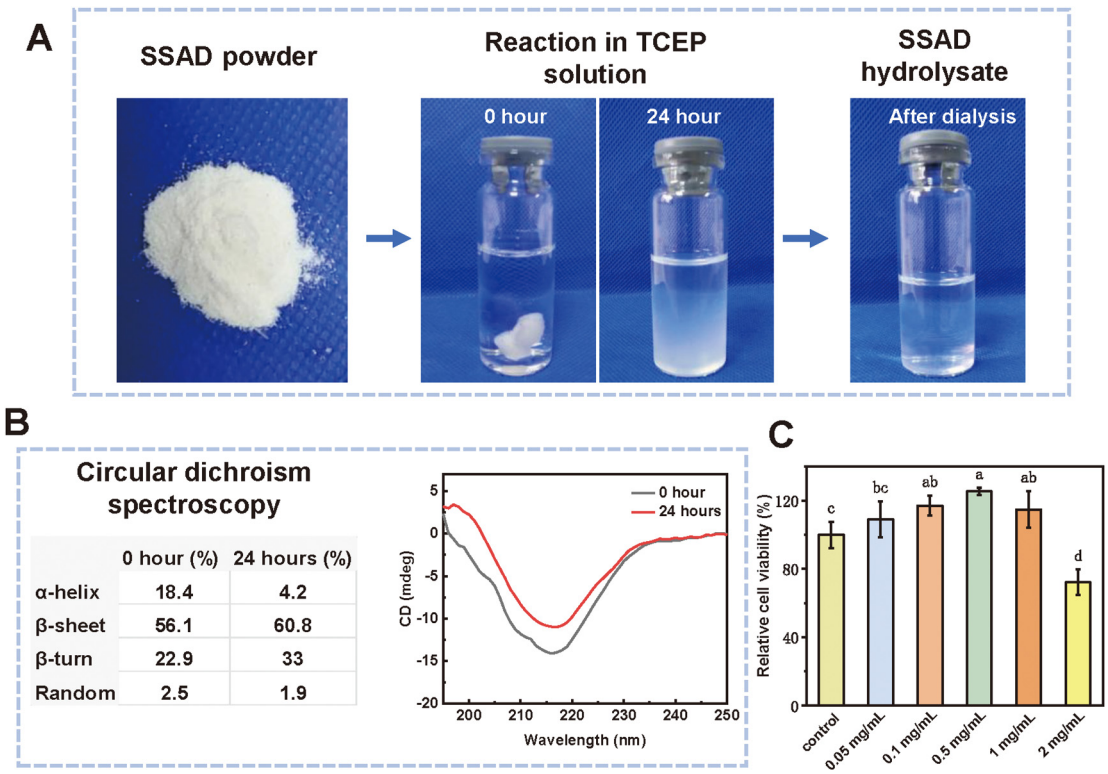

Fig. 1 Preparation of SSAD hydrolysate (A). Circular dichroism analysis of SSAD hydrolysate before and after tris(2-carboxyethyl)phosphine (TCEP) treatment (B). Cell counting kit-8 (CCK-8) results of SSAD hydrolysate cultured with human dental pulp stem cells (HDPSCs) (C). Different letters denote significant differences ($n = 6$, $p < 0.05$).

Circular dichroic spectroscopy was used to analyze the secondary protein structure in SSAD before and after TCEP treatment. The results (Fig. 1(B)) indicated that the relative content of the protein secondary structure in SSAD changed after TCEP treatment and that the hydrolysate was rich in β-sheet structures. Specifically, the relative content of the β-sheet in the SSAD hydrolysate increased from 56.1% to 60.8%, while that of the β-turn increased from 22.9% to 33.0%. The relative content of the α-helix decreased from 18.4% to 4.2%, while that of the random coil decreased from 2.5% to 1.9%.

In this experiment, the cytotoxicity of SSAD hydrolysate toward HDPSCs was evaluated using the CCK-8 assay. As shown in Fig. 1(C), 2 mg mL^{-1} of SSAD hydrolysate exhibited an inhibitory effect on cell growth, whereas SSAD hydrolysates at concentrations of 1, 0.5, and 0.1 mg mL^{-1} exhibited promotional effects on cell growth. The cell viability in the 0.05 mg mL^{-1} group was not significantly different compared with the control group. Among the tested concentrations, the 0.5 mg mL^{-1} group exhibited the most pronounced effect on cell growth.

3.2. Effects of different SSAD hydrolysate concentrations on dentin remineralization

Dentin specimens were prepared and treated as shown in Fig. 2(A). FESEM images of intact dentin showed inter-tubular and peritubular dentin with minerals. After acid etching with EDTA, the dentinal tubules were opened, and collagen fibrils were exposed (Fig. S2, ESI†). To investigate the effects of different concentrations of SSAD hydrolysate on dentin remineralization, we applied SSAD hydrolysate to acid-etched dentin at concentrations of 0.05, 0.1, 0.5, 1, and 2 mg mL^{-1}. The dentin samples were then incubated in AS for 1 week.

FESEM observation revealed obvious differences in the dentin surface morphology and remineralization effect among the different SSAD hydrolysate concentration groups (Fig. 2(B)). At a concentration of 2 mg mL^{-1}, SSAD hydrolysate agglomerated on the dentin surface, forming sheet-like deposits around the collagen fibrils. At a concentration of 1 mg mL^{-1}, SSAD hydrolysate was distributed as different-sized particles on the dentin surface, with some areas still showing agglomeration. At a concentration of 0.5 mg mL^{-1}, SSAD hydrolysate was uniformly dispersed on the dentin surface as nanometer-sized spherical particles, and the collagen fibrils remained fluffy without obvious collapse. At a concentration of 0.1 mg mL^{-1}, SSAD hydrolysate was uniformly distributed on the dentin surface, but the nanoparticles formed were smaller than those in the 0.5 mg mL^{-1} group, and focal collagen collapse was observed. At a concentration of 0.05 mg mL^{-1}, SSAD hydrolysate showed no nanoparticle deposition on the dentin surface, and the collagen fibrils collapsed. After 1 week of remineralization, the 0.5 mg mL^{-1} group exhibited the most obvious mineral deposition.

FESEM was used to observe the dentin coated with 0.5 mg mL^{-1} SSAD hydrolysate before and after ultrasonication. As shown in Fig. 2(C), before ultrasonic treatment, the SSAD hydrolysate was uniformly distributed on the collagen fibrils, keeping the fibrils fluffy. After ultrasonic treatment, although the SSAD hydrolysate exfoliated in some regions, a significant number of nanoparticles were still discernible, indicating that the SSAD hydrolysate had a certain bonding capacity to collagen fibrils. The contact angles of the dentin surface were measured after treatment with different concentrations of SSAD hydrolysate. As shown in Fig. 2(D), the contact angles of the dentin surface in the 2 and 1 mg mL^{-1} groups were significantly higher than those of the other groups ($p < 0.05$), while there was no significant difference among the 0.5, 0.1, and 0.05 mg mL^{-1} groups. These results suggest that high concentrations of SSAD hydrolysate (1 mg mL^{-1} and 2 mg mL^{-1}) decreased the hydrophilicity of the dentin surface, whereas concentrations lower than 0.5 mg mL^{-1} had no obvious effect on its hydrophilicity.

3.3. Intrafibrillar collagen mineralization

The effect of SSAD hydrolysate on collagen fibril mineralization was evaluated using reconstituted type I collagen. Calcium and phosphorus ions in the control group formed needle-shaped crystals after incubation in AS for 6 h (as shown by the white arrow in Fig. 3(A)). There was no significant difference after 12-h and 24-h incubations in the control group. The electron densities of the collagen fibrils were low, and HA crystal particles were visible in the solution (Fig. 3(A1) and (A2)). In the SSAD group, after 6 h of incubation, Ca and P ions in the solution were in an amorphous state (as shown by the white arrow in Fig. 3(B)), and no obvious crystal particles were formed. After 12 h of incubation, needle-shaped crystals were detected around the collagen fibrils (Fig. 3(B1)). After 24 h of incubation, the electron density of collagen fibrils increased (Fig. 3(B2)). TEM observations showed that calcium and phosphorus ions in the SSAD hydrolysate remained amorphous, whereas those in the control group rapidly crystallized. According to the theory of dentin bionic mineralization, SSAD hydrolysate might be able to stabilize calcium and phosphorus ions and induce their flow into collagen fibrils, thereby promoting mineralization within collagen fibrils.[36,37] During the mineralization reaction of recombinant type I collagen, calcium and phosphorus ions preferentially accumulated around the collagen fiber surfaces in the SSAD-treated group.

3.4. Characterization of dentinal tubule occlusion

To further investigate the effects of dentinal tubule occlusion and remineralization induced by SSAD hydrolysate, the acid-etched dentin slices treated with 0.5 mg mL^{-1} SSAD hydrolysate (SSAD group) and deionized water (as control) were incubated in AS for 1, 2, and 4 weeks, before examining the morphology of the dentin samples using FESEM (Fig. 3(C)).

In the control group, no significant increase in minerals was observed on the dentin surface after 1 week of remineralization. After 2 weeks, minimal amounts of mineral particles began to accumulate on the dentin surface. By 4 weeks, the quantity of mineral deposits increased but remained unevenly distributed, and numerous dentinal tubules were still exposed. No substantial mineral deposition was noted within the dentinal tubules at

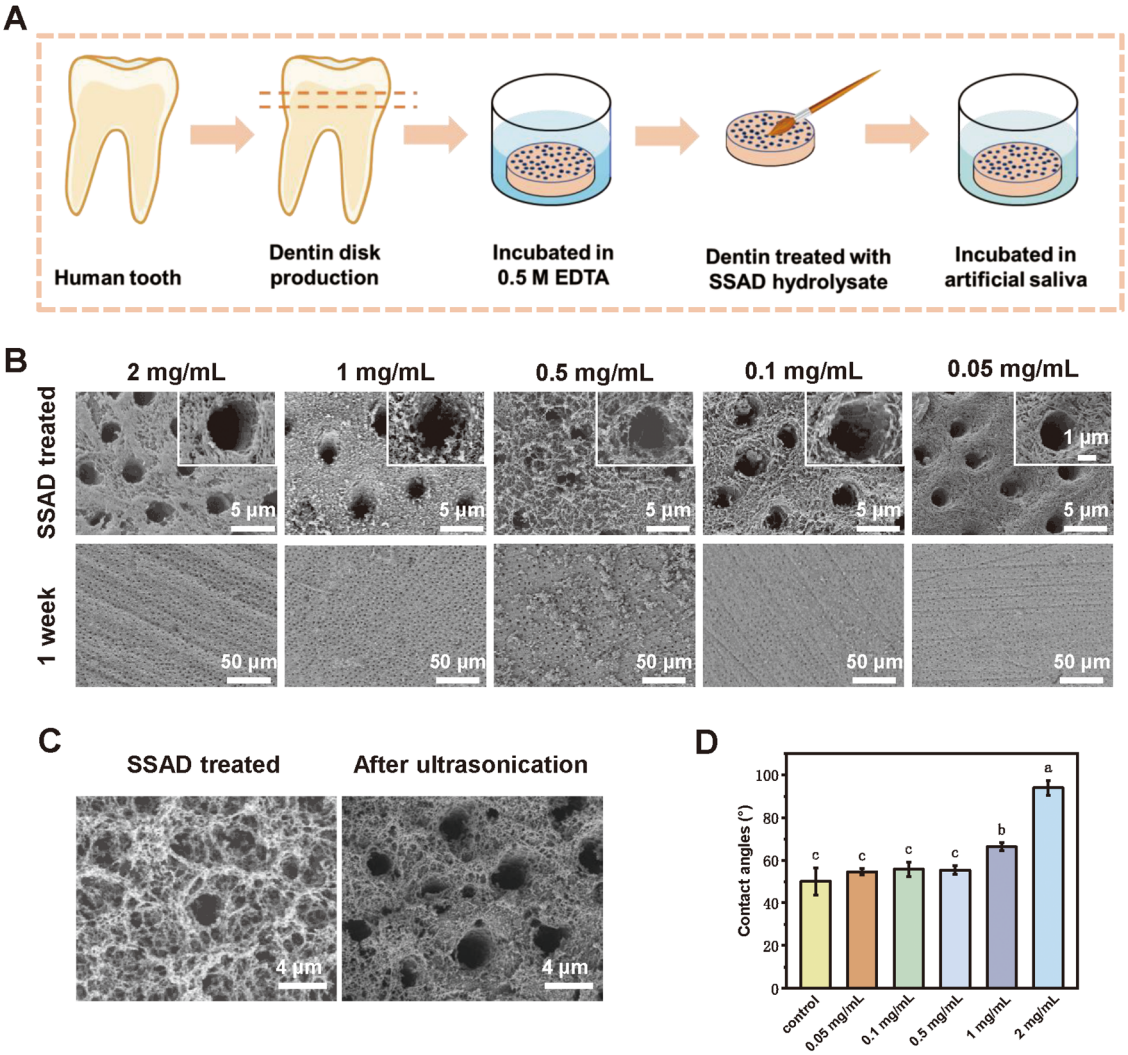

Fig. 2 Schematic illustration of dentin specimen preparation and treatment (A). FESEM images of the dentin surface after treatment with different concentrations of SSAD hydrolysate and after remineralization for 1 week (B). FESEM images of the dentin surface treated with 0.5 mg mL^{-1} SSAD hydrolysate before and after ultrasonication (C). Contact angle examination of the dentin surface after treatment with different concentrations of SSAD hydrolysate (D). Different letters denote significant differences (n = 5, $p < 0.05$).

any time point during the remineralization period. In contrast, in the SSAD group, small amounts of mineral particles were deposited around the SSAD hydrolysate on the dentin surface after 1 week of remineralization. After 2 weeks, the amount of deposits increased significantly both on the surface and in the dentinal tubules, with a more uniform distribution and reduced tubule diameter. By 4 weeks, the dentinal tubule orifices were almost entirely sealed by nanoscale minerals, and cross-sectional observations revealed mineral deposits within the dentinal tubules. As the remineralization reaction progressed, the density of deposits within the tubules gradually increased, nearly filling the dentinal tubules by the fourth week. These findings suggest that SSAD hydrolysate can effectively induce mineral deposition on the dentin surface and within the dentinal tubules, resulting in the deep occlusion of dentinal tubules over time. The depth of dentinal tubule mineralization was up to 30 ± 5 μm (Fig. 3(D)).

As shown in Fig. S3A (ESI†), the FESEM results revealed the formation of a uniform coating on the dentin surface after Duraphat application, with complete occlusion of dentinal tubules and an occlusion depth of 5–8 μm (Fig. S3B, ESI†). The Duraphat coating on the surface can be easily peeled off after ultrasonic treatment (Fig. S3C, ESI†), and, as a result, the dentinal tubules were empty. For the Gluma group, no change could be observed on the surface and cross-sectional views of the dentin surface (Fig. S4, ESI†).

EDX analysis of the dentin surface after 4-week mineralization revealed a calcium–phosphorus ratio of 1.64, closely resembling that of natural HA (Fig. 3(E) and (F)).[38,39] XRD analysis was used to characterize the mineral phase of precipitates on dentin samples. As illustrated in Fig. 3(G), untreated dentin exhibited distinct HA diffraction peaks at 2θ angles of 25.9° (002), 31.8° (211), and 32.9° (300).[40] These peaks are characteristic of the crystalline structure of HA, a major

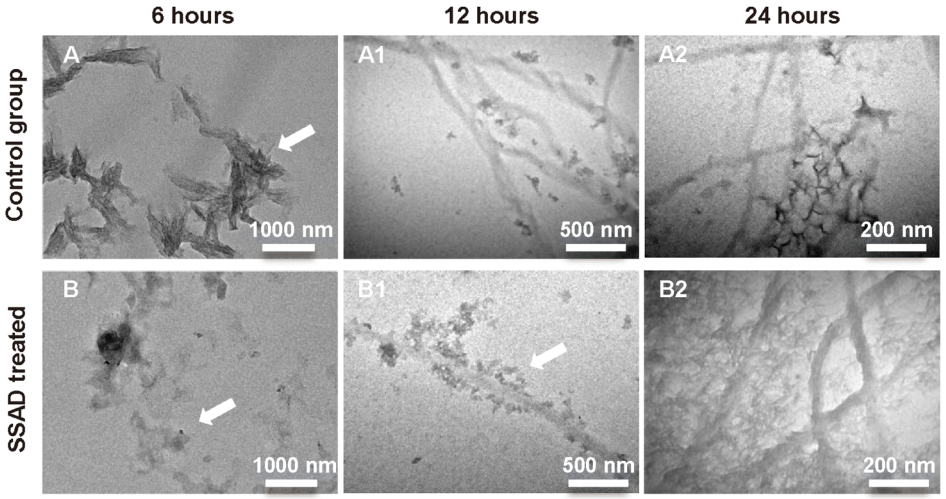

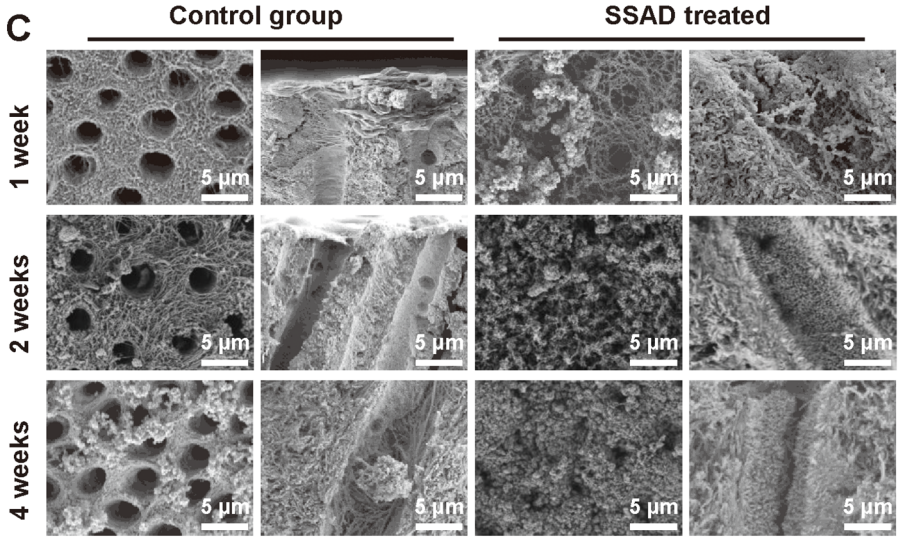

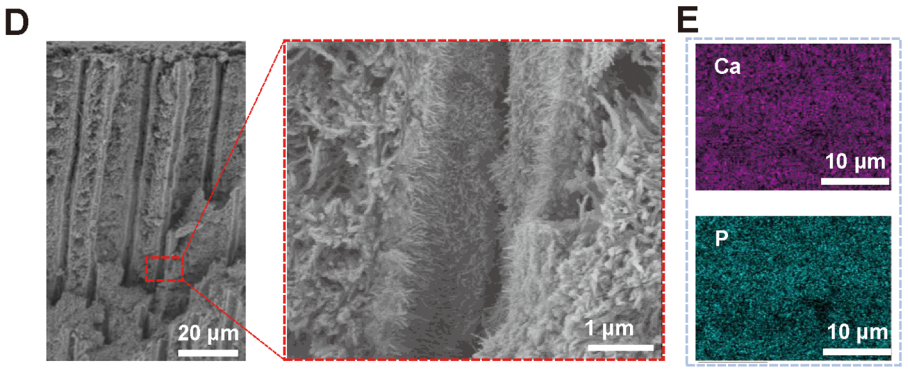

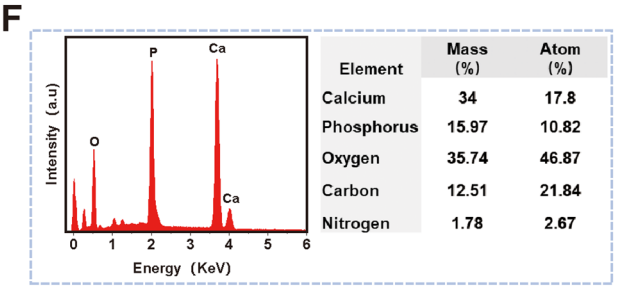

Element	Mass (%)	Atom (%)
Calcium	34	17.8
Phosphorus	15.97	10.82
Oxygen	35.74	46.87
Carbon	12.51	21.84
Nitrogen	1.78	2.67

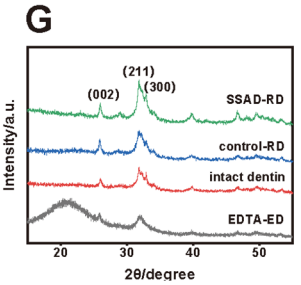

Fig. 3 TEM images of the remineralization of reconstructed type I collagen in the control and SSAD hydrolysate groups during different periods (A) and (B). FESEM images of dentin remineralized for 1, 2, and 4 weeks (C). FESEM images of the cross-section of SSAD-treated dentin remineralized for 4 weeks, and the high magnification FESEM image showing mineralized crystal deposited at a depth of 30 ± 5 μm (D). EDX results of the crystals on the surface of SSAD-treated dentin remineralized for 4 weeks (E) and (F). XRD analysis of intact dentin, EDTA-etched demineralized dentin (EDTA-ED), and remineralized dentin (RD) in SSAD and control group for 4 weeks (G).

component of dentin.[35] After the EDTA acid-etched process, most of the characteristic HA peaks showed a substantial reduction in intensity, indicating the loss of HA in dentin. The broadened peak widths suggested a decrease in crystallinity.[41,42] In contrast, after 4-week remineralization, the dentin in the SSAD group showed characteristic HA diffraction peaks. The peaks were higher and the widths were narrower than those in the control group. The enhanced crystallinity of the SSAD group verified its effective remineralization and crystal-forming capacity.

Resistance to oral acid exposure is an important evaluation standard for desensitizers in the clinical treatment of dentin hypersensitivity.[10,34] Citric acid was used for anti-acid evaluation to further explore the long-term stability of tubule occlusion induced by SSAD hydrolysate.[43] As shown by FESEM in Fig. 4(A), after acid exposure in citric acid, the remineralized dentin in the control group exhibited exposed dentinal tubules and a mineral-free dentin surface, whereas the dentinal tubules in the SSAD hydrolysate group remained plugged with deposits.

Dentin permeability evaluation is often considered the "gold standard" for appraising the dentin occlusion capacity.[44] As shown in Fig. 4(B), the SSAD and control groups showed significant differences in dentin permeability, both after 4-week remineralization and after acid challenge. After remineralization, the SSAD group exhibited a notable decrease in Lp% values compared with the control group, which was consistent with the excellent tubule occlusion observed using FESEM. Acid challenge may lead to the loss of minerals, resulting in higher dentin permeability. After citric acid challenge, the Lp% value of the SSAD group increased from 21.07% to 38.52% but remained significantly lower than that of the control groups ($p < 0.001$). In summary, although acid challenge increased the permeability in all groups, the SSAD group maintained lower Lp% values than the control groups, highlighting its effectiveness in reducing dentin permeability even under acidic conditions.

Fig. 4(C) shows the mean ± SD of surface microhardness for groups at various time points. The microhardness of EDTA-

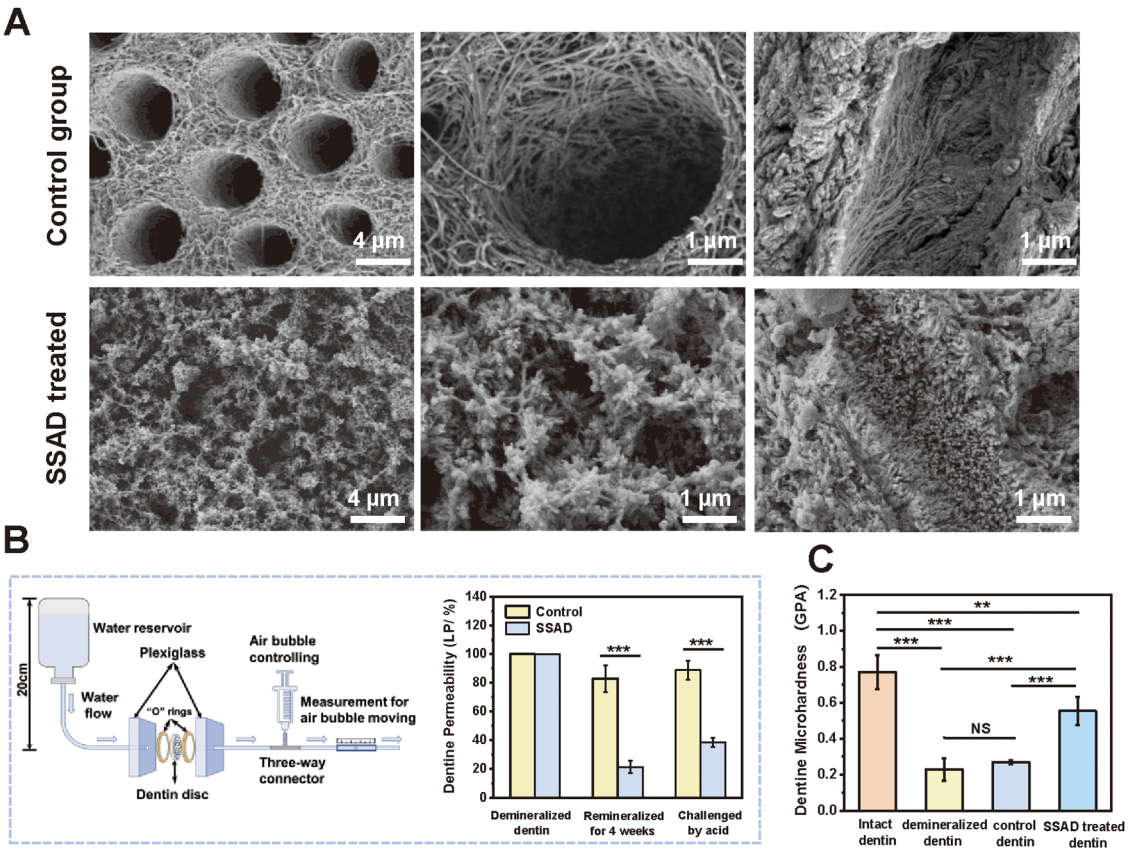

Fig. 4 FESEM images of remineralized dentin samples subjected to citric acid challenge (A). Schematic of the equipment used for the dentin permeability assay and dentin permeability (Lp%) data in different groups (B) (n = 6, ***$p < 0.001$). Dentin microhardness measurement (C) of intact dentin, EDTA-etched dentin, and dentin after 4 weeks of remineralization (n = 5; ns: not significant, **$p < 0.01$, and ***$p < 0.001$).

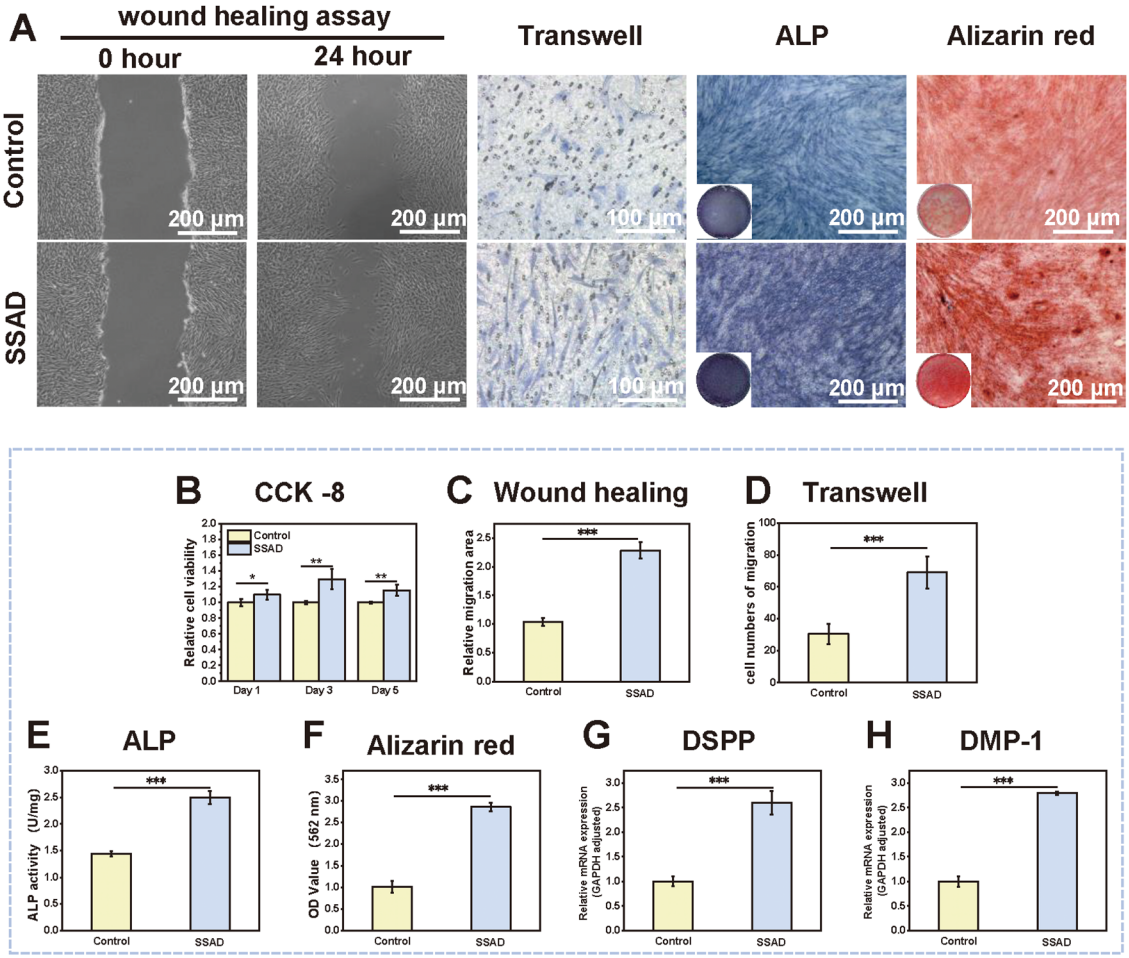

Fig. 5 Role of SSAD hydrolysate in the proliferation, migration, and osteogenic and odontogenic differentiation of HDPSCs *in vitro*. Microscopic images of the wound healing assay, transwell assay, and ALP and alizarin red staining of HDPSCs (A). CCK-8 assay (B) of HDPSCs cultured with SSAD hydrolysate for 1, 3, and 5 days (n = 6; *p < 0.05 and **p < 0.01). Quantitative analysis of the wound healing assay (C), (n = 5) transwell assay (D), (n = 6), and ALP activity (E), (n = 3); semi-quantitative analysis of alizarin red staining (F), (n = 3); qRT-PCR assay of odontogenic-related gene expression (G) and (H), (n = 6) of HDPSCs cultured with or without SSAD hydrolysate (***p < 0.001).

etched dentin (0.228 ± 0.06 GPa) was significantly lower than that of intact dentin (0.771 ± 0.094 GPa). After 4 weeks of remineralization, the dentin microhardness in the SSAD hydrolysate group was (0.554 ± 0.08 GPa), representing a significant increase compared with the control group (0.267 ± 0.01 GPa). The microhardness value of the SSAD group was slightly lower than that of the intact dentin, which suggests that although remineralization with SSAD hydrolysate improved the microhardness, it did not completely restore the dentin to its original state.

3.5. Biosafety research

In our experiment, the concentration of SSAD hydrolysate that induced dentin remineralization and dentinal tubule occlusion was 0.5 mg mL^{-1}. We selected this concentration to further explore its effect on HDPSCs. The CCK-8 results in Fig. 5(B) show that compared with the control group, the relative cell vitality of the SSAD hydrolysate (0.5 mg mL^{-1}) group was significantly increased on days 1, 3, and 5. These results indicate that SSAD hydrolysate (0.5 mg mL^{-1}) can promote the proliferation of HDPSCs.

Cell scratch tests and transwell migration assays were performed to evaluate the effects of SSAD hydrolysate on the migration of HDPSCs. As depicted in Fig. 5(A, C and D), the migration area and number of migrated cells of the SSAD hydrolysate group were significantly greater than those of the control group.

To verify the osteogenic effects of SSAD hydrolysate on HDPSCs, we performed ALP staining, alizarin red staining, and quantitative assays.[45] After 14 days of induction in OI medium, ALP staining revealed that the stained area of cells in the SSAD group was larger than that of the control group (Fig. 5(A)), indicating early osteogenic effects.[46] Consistent with the quantitative results of ALP cell lysates, the ALP activity was higher in the SSAD group than in the control group (Fig. 5(E)). The results of alizarin red staining and the quantitative assay (Fig. 5(A) and (F)) showed that the number of calcium nodules in the SSAD hydrolysate-treated group was significantly increased compared with the control group.

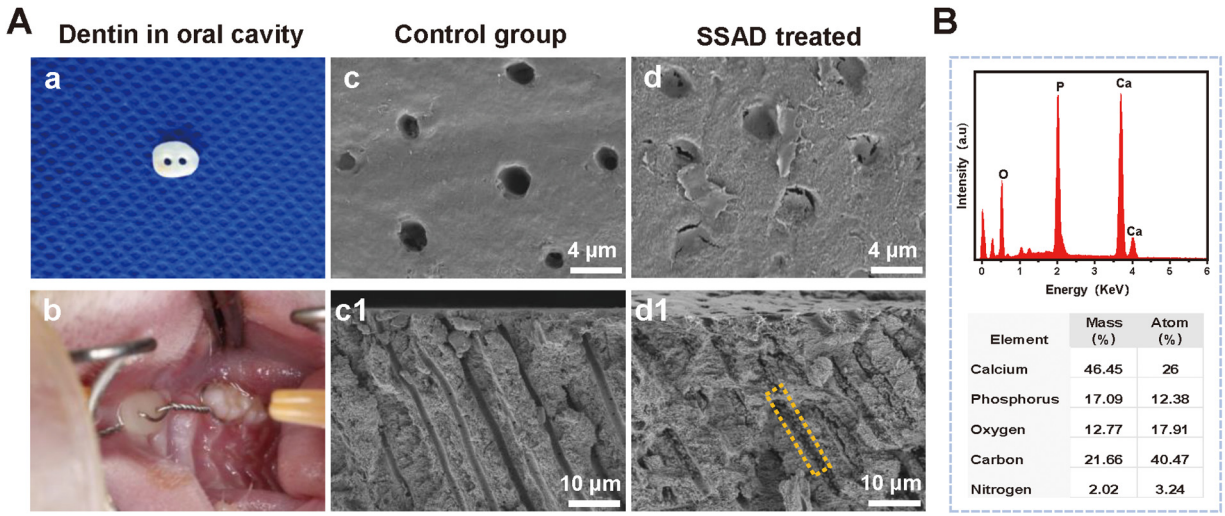

Fig. 6 *In vivo* animal experiments of dentinal tubule occlusion in the oral cavity of SD rats (A). Preparation (a) and fixation (b) of dentin disks in the oral cavity of SD rats. FESEM images of dentin samples after incubation for 4 weeks in the oral cavity of SD rats (c, c1, d, and d1). EDX analysis of the dentinal tubule dotted with yellow boxes (B).

DSPP and *DMP-1* are key indicators of dentin matrix mineralization.[47] These genes play crucial roles in regulating calcium and phosphate metabolism, thus affecting the initiation and maturation of dentin mineralization. According to qRT-PCR, the mRNA expression of both *DSPP* and *DMP-1* was significantly upregulated in the SSAD group after 7 days of cultivation (Fig. 5(G) and (H)) compared with the control group, demonstrating promising odontogenic efficacy. In summary, our results confirmed that at a concentration of 0.5 mg mL^{-1}, SSAD hydrolysate can promote cell proliferation, migration, and odontogenic differentiation of HDPSCs.

3.6. Animal experiments

For further clinical application, *in vivo* experiments were designed. The dentin disk was first treated with or without 0.5 mg mL^{-1} SSAD hydrolysate and then fixed on the teeth of SD rats, as shown in Fig. 6(A)-a and b.[48,49] In the control group, the dentinal tubules were still open after a 4-week incubation (Fig. 6(A)-c and c1), whereas the dentinal tubules of the SSAD hydrolysate groups were completely occluded (Fig. 6(A)-d and d1), and the deposited minerals could be observed deep in the tubules to approximately 30 μm. As shown by the EDX (Fig. 6(B)), the Ca/P ratio of minerals in the dentinal tubules was 2.16, slightly higher than that in HA (Ca/P 1.67), which may be due to the mixture of impurities such as calcium oxide. Thus, the *in vivo* experiments indicated that SSAD hydrolysate facilitates oral remineralization of dentin and dentinal tubule occlusion.

4. Discussion

In this research, we describe the application of SSAD hydrolysate to induce dentin remineralization and dentinal tubule occlusion. We used TCEP to successfully reduce disulfide linkages in proteins, thereby producing SSAD hydrolysate. Protein spatial conformation is predominantly maintained by intramolecular hydrogen bonds and disulfide bonds.[50] TCEP, with its high selectivity for reducing disulfide bonds, has been previously used by Li *et al.* to prepare nanoscale amyloid aggregates by reducing the intramolecular disulfide bond of lysozyme.[16] Prior research has shown that when SSAD powder is hydrated, numerous disulfide bonds are generated.[20] These dynamic covalent disulfide bonds have found extensive applications in biomaterial creation.[51–53] SSAD protein has an abundance of α-helix structures, which are likely stabilized by intramolecular S–S bonds. As shown by circular dichroic spectroscopy, with TECP reduction, the relative content of the α-helix decreased, and the relative content of the β-sheet and β-turn in the SSAD hydrolysate increased. If the S–S bonds are reduced, the α-helix transitions swiftly, leading to the rapid formation of β-sheet-rich amyloid oligomers and protofibrils in minutes.[54–56]

Compared with SSAD powder or hydrogel, SSAD hydrolysate exhibits enhanced fluidity, which enables it to more easily penetrate the gaps between collagen fibers and dentinal tubules. After reduction with TCEP, SSAD hydrolysate exposes various functional groups, including amine, guanidyl, carboxyl, and hydroxyl groups, all of which play a crucial role in facilitating stable interfacial adhesion to the demineralized dentin matrix.[26] FESEM analysis before and after ultrasonication confirmed that 0.5 mg mL^{-1} SSAD hydrolysate forms a robust and stable bond with collagen fibrils, providing favorable conditions for subsequent dentin remineralization.

The concentration of SSAD hydrolysate significantly affects its performance. The FESEM results indicated that at higher concentrations (1 mg mL^{-1} and 2 mg mL^{-1}), SSAD hydrolysates tend to agglomerate, which can impede their penetration into dentinal tubules. In contrast, 0.5 mg mL^{-1} of SSAD hydrolysate was uniformly distributed as nanoparticles with a diameter of

approximately 60 nm on the collagen fibrils, while concentrations lower than 0.05 mg mL^{-1} had little effect on the dentin surface topography. High-concentration hydrolysate agglomeration on the dentin surface can increase surface tension and reduce dentin surface hydrophilicity, as evidenced by contact angle measurements. Because surface energy and surface wettability are correlated and can be objectively reflected by surface contact angle measurements,[57] smaller contact angles indicate better surface wettability, which is vital for the reaction between coating materials and the dentin matrix. Agglomeration is unfavorable for calcium and phosphorus ion binding, whereas lower-concentration hydrolysates lack sufficient functional components, weakening their ability to induce calcium and phosphorus ion accumulation. In contrast, hydrolysate at a concentration of 0.5 mg mL^{-1} can evenly distribute around the collagen fibrils in the form of nanoscale particles with uniform porosity, effectively promoting calcium and phosphorus deposition.

To further explore the dentin remineralization and dentinal tubule-sealing processes, the acid-etched dentin disks treated with 0.5 mg mL^{-1} SSAD hydrolysate or deionized water were incubated in AS for 1, 2, and 4 weeks. After 4 weeks of mineralization, the results showed that the dentinal tubules in the control group remained open and that the mineral particles even disappeared after acid challenge. However, in the SSAD hydrolysate treatment group, a large number of minerals were deposited on the dentin surface and deep into the tubules after 4 weeks of mineralization. Consequently, the dentinal tubules were occluded, the dentin permeability decreased, and minerals were retained even after citric acid challenge. This approach provides a promising foundation for the treatment of dentin hypersensitivity. Duraphat and Gluma desensitizer, as commonly used agents for treating dentin hypersensitivity, were chosen as positive controls. As shown by FESEM, Duraphat varnish could occlude the dentinal tubules but was unstable in response to ultrasonic challenge, possibly attributed to the lack of stable adhesion between the varnish and the dentin. Gluma alleviated dentin hypersensitivity through the reaction of protein coagulation, but the dentinal tubules remained open after Gluma treatment. In comparison, dentinal tubule occlusion mediated by SSAD-induced dentin remineralization was associated with more pronounced and long-lasting efficacy. The combined results of FESEM and TEM suggest that SSAD hydrolysate may function similarly to NCPs, with dual roles of adhering to collagen fibrils and stabilizing calcium and phosphorus ions.[44] This dual function provides the necessary conditions for collagen fibril mineralization. Although the exact mechanism by which SSAD hydrolysate induces dentin remineralization is unclear, the negatively charged amino acids in the SSAD hydrolysate could interact electrostatically with positively charged calcium ions, and the secondary structures (including α-helices and β-sheets) present in the hydrolyzed peptides might provide additional binding sites for mineral deposition.

Based on the pulp-dentin complex, external stimuli can elicit biodefense and inflammatory responses from dental pulp stem cells under various conditions.[32,58–60] Therefore, materials used on dentinal tubules must possess excellent biocompatibility.[61] A material that induces odontogenesis and mineralization of dental pulp stem cells is crucial for the long-term treatment of dentin hypersensitivity. To this end, *in vitro* cellular experiments were conducted to evaluate the effect of SSAD hydrolysate on HDPSCs. The *in vitro* results demonstrated that SSAD hydrolysate exhibited good biocompatibility and promoted the proliferation, migration, and osteogenic and odontogenic differentiation of HDPSCs. Previous research has verified that a bioactive hydrogel derived from SSAD hydrolysate, which was developed for bone regeneration, can stimulate signaling pathways related to osteogenesis.[26] SSAD hydrogels are known to provide glycine during collagen synthesis and release insulin-like growth factor-1 and stromal cell-derived factor-1, both of which could contribute to enhancing cell proliferation and collagen production.[22] Thus, the effect of SSAD hydrolysate on the induction of osteogenic and odontogenesis differentiation of HDPSCs may be associated with the coordination of abundant growth factors, appropriate chemical composition, and functional peptide components within the SSAD hydrolysate.

According to the results of *in vitro* and *in vivo* experiments, SSAD hydrolysate represents a safe and effective dentin desensitization agent. However, given the complex intra-oral environment, the clinical application of SSAD hydrolysate must endure the challenges posed by saliva and chewing. Therefore, clinical research is essential before its clinical translation. While the sample size was justified by prior research, formal power analysis was not conducted. Future studies with larger cohorts and multivariate analyses are warranted to further validate these findings. To address ethical and ecological concerns, we are attempting to isolate the effective components of SSAD and extract active polypeptides, with the expectation of using biosynthesis as an alternative approach to achieve more efficient clinical applications.

5. Conclusion

In this study, we successfully obtained SSAD hydrolysate by reducing it with TCEP and innovatively applied it to induce dentin remineralization and dentinal tubule occlusion. First, the hydrolysate could effectively bind to the dentin collagen matrix, forming nanoscale agglomerates and promoting the aggregation of Ca and P ions. Second, after reacting in AS for 4 weeks, the application of SSAD hydrolysate significantly induced dentin remineralization and occluded dentinal tubules. The remineralized dentin exhibited excellent acid stability, the permeability of the dentinal tubules was markedly reduced, and the microhardness of acid-etched dentin was notably improved. Furthermore, SSAD hydrolysate demonstrated good biocompatibility and promoted the proliferation, migration, and osteogenic and odontogenic differentiation of HDPSCs. Animal studies also showed that the dentinal tubules were completely blocked after treatment with SSAD hydrolysate. Therefore, SSAD hydrolysate has great potential in the

management of dentin hypersensitivity, and further randomized clinical trials are warranted.

Author contributions

Yongxiang Zeng: data curation, formal analysis, investigation, methodology, validation, visualization, writing – original draft. Lin Yang: data curation, formal analysis, investigation, validation, visualization, writing – review & editing. Na Wu: data curation, formal analysis, investigation, validation, visualization, writing – review & editing. Hong Chen: data curation, investigation, methodology, visualization, writing – review & editing. Ximu Zhang: conceptualization, data curation, funding acquisition, supervision, visualization, writing – review & editing. Deqin Yang: conceptualization, data curation, funding acquisition, supervision, visualization, writing – review & editing.

Conflicts of interest

The authors declare that they have no known competing financial interests or personal relationships that could have appeared to influence the work reported in this paper.

Data availability

All data supporting the findings of this study, including the data for figures and tables, are included within the article.

Acknowledgements

This work was supported by funding from the National Natural Science Foundation of China (no. 32270888), the First Batch Scientific and Technological Innovation Key Project at Chongqing Medical University (no. 2023 (157)), Chongqing Natural Science Foundation Innovation and Development Joint Fund (Municipal Education Commission) Project (no. CSTB2022NSCQ-LZX0039), Outstanding Youth Fund of Chongqing Natural Science Foundation (CSTB2023NSCQ-JQX0006) and Science and Technology Research Project of Chongqing Education Commission (KJQN202200471).

References

1 H. J. Shiau, *J. Evid. Based Dent. Pract.*, 2012, **12**, 220–228.
2 M. Addy, *Int. Dent. J.*, 2002, **52**, 367–375.
3 L. Favaro Zeola, P. V. Soares and J. Cunha-Cruz, *J. Dent.*, 2019, **81**, 1–6.
4 K. Bekes, M. John, H. G. Schaller and C. Hirsch, *J. Oral Rehabil.*, 2009, **36**, 45–51.
5 M. Brännström, *Odontol. Revy*, 1965, **16**, 293–299.
6 D. Clark and L. Levin, *Int. Dent. J.*, 2016, **66**, 249–256.
7 J. Creeth, J. Gallob, F. Sufi, J. Qaqish, P. Gomez-Pereira, C. Budhawant and C. J. B. O. H. Goyal, *BMC Oral Health*, 2019, **19**, 1–9.
8 G. Craig, G. Knight and J. M. McIntyre, *Aust. Dent. J.*, 2012, **57**, 308–311.
9 I. Willershausen, D. Schulte, A. Azaripour, V. Weyer-Elberich, B. Briseno and B. Willershausen, *Clin. Lab.*, 2015, **61**, 1695–1701.
10 Q. Wang, J. Luan, Z. Zhao, W. Kong, C. Zhang and J. Ding, *Chin. Chem. Lett.*, 2023, **34**, 108060.
11 M. Wang, H. Deng, T. Jiang and Y. Wang, *Biomater. Adv.*, 2022, **135**, 112670.
12 Y. Qu, T. Gu, Q. Du, C. Shao, J. Wang, B. Jin, W. Kong, J. Sun, C. Chen, H. Pan, R. Tang and X. Gu, *ACS Biomater. Sci. Eng.*, 2020, **6**, 3327–3334.
13 B. Yang, G. Chen, J. Li, Q. Zou, D. Xie, Y. Chen, H. Wang, X. Zheng, J. Long and W. J. B. Tang, *Biomaterials*, 2012, **33**, 2449–2461.
14 J. Yang, J. Huang, H. Qin, J. Long, X. Lin and F. Xie, *J. Biomater. Sci., Polym. Ed.*, 2022, **33**, 668–686.
15 Y. Wen, J. Wang, J. Luo and J. Yang, *Heliyon*, 2020, **6**, e05886.
16 C. Li, D. Lu, J. Deng, X. Zhang and P. Yang, *Adv. Mater.*, 2019, **31**, e1903973.
17 Y. Xu, J. Guan, Q. Wang, R. Xue, Z. He, X. Lu, J. Fan, H. Yu, C. Turghun, W. Yu, Z. Li, S. Abay, W. Chen and B. Han, *ACS Appl. Mater. Interfaces*, 2023, **15**, 15946–15964.
18 B. Saravana Karthikeyan and S. Mahalaxmi, *Int. J. Biol. Macromol.*, 2024, **270**, 132359.
19 S. V. Aruna Rani, K. Rajkumar, B. Saravana Karthikeyan, S. Mahalaxmi, G. Rajkumar and V. Dhivya, *J. Mech. Behav. Biomed. Mater.*, 2023, **141**, 105748.
20 J. Deng, Y. Tang, Q. Zhang, C. Wang, M. Liao, P. Ji, J. Song, G. Luo, L. Chen, X. Ran, Z. Wei, L. Zheng, R. Dang, X. Liu, H. Zhang, Y. S. Zhang, X. Zhang and H. Tan, *Adv. Funct. Mater.*, 2019, **29**, 1809110–1809123.
21 X. Geng, H. Wei, H. Shang, M. Zhou, B. Chen, F. Zhang, X. Zang, P. Li, J. Sun, J. Che, Y. Zhang and C. Xu, *J. Proteomics*, 2015, **119**, 196–208.
22 R. Dang, L. Chen, F. Sefat, X. Li, S. Liu, X. Yuan, X. Ning, Y. S. Zhang, P. Ji and X. Zhang, *Small*, 2022, **18**, 2105255.
23 Y. Yan, J. Huang, X. Qiu, D. Zhuang, H. Liu, C. Huang, X. Wu and X. Cui, *Chem. Eng. J.*, 2022, **431**, 133460.
24 B. K. Ahn, *J. Am. Chem. Soc.*, 2017, **139**, 10166–10171.
25 P. Kord Forooshani and B. P. Lee, *J. Polym. Sci., Part A: Polym. Chem.*, 2017, **55**, 9–33.
26 Q. Zhang, X. Feng, S. Peng, L. Li, Y. Xiang, T. Feng, X. Zhang and J. Song, *Composites, Part B*, 2024, **274**, 111261.
27 X. Zhang, L. Jiang, X. Li, L. Zheng, R. Dang, X. Liu, X. Wang, L. Chen, Y. S. Zhang and J. J. S. Zhang, *Small*, 2022, **18**, 2101699.
28 S. Liu, Y. Xiang, Z. Liu, L. Li, R. Dang, H. Zhang, F. Wei, Y. Chen, X. Yang, M. Mao, Y. S. Zhang, J. Song and X. Zhang, *Adv. Mater.*, 2024, **36**, 2309774.
29 K. Liang, M. D. Weir, X. Xie, L. Wang, M. A. Reynolds, J. Li and H. H. Xu, *Dent. Mater.*, 2016, **32**, 1429–1440.
30 K. Liang, S. Xiao, H. Liu, W. Shi, J. Li, Y. Gao, L. He, X. Zhou and J. Li, *Dent. Mater.*, 2018, **34**, 629–640.

31 J. Yu, H. Yang, K. Li, H. Ren, J. Lei and C. Huang, *ACS Appl. Mater. Interfaces*, 2017, **9**, 25796–25807.
32 J. Yu, H. Bian, Y. Zhao, J. Guo, C. Yao, H. Liu, Y. Shen, H. Yang and C. Huang, *Bioact. Mater.*, 2023, **23**, 394–408.
33 X. Qiao, J. Tang, L. Dou, S. Yang, Y. Sun, H. Mao and D. Yang, *Int. J. Nanomed.*, 2023, 4683–4703.
34 Y. Xu, X. Pan, D. Shen, Y. Sun, W. Liu, Y. Lin, B. Fu and L. Zhang, *Int. J. Biol. Macromol.*, 2024, **254**, 127780.
35 J. He, J. Yang, M. Li, Y. Li, Y. Pang, J. Deng, X. Zhang and W. Liu, *ACS Nano*, 2022, **16**, 3119–3134.
36 L. N. Niu, W. Zhang, D. H. Pashley, L. Breschi, J. Mao, J. H. Chen and F. R. Tay, *Dent. Mater.*, 2014, **30**, 77–96.
37 F. Nudelman, A. J. Lausch, N. A. Sommerdijk and E. D. Sone, *J. Struct. Biol.*, 2013, **183**, 258–269.
38 L. Meng, M. Shu, P. Mei, Y. Liang and L. J. B. O. H. Xia, *BMC Oral Health*, 2025, **25**, 204.
39 L. K. R. d Oliveira, C. D. d Nascimento Neto, A. B. Costa e Silva, S. M. W. Rocha, P. R. Bianchi, A. G. d S. Galdino and D. N. J. C. O. I. Silva, *Clin. Oral Investig.*, 2025, **29**, 1–15.
40 J. Reyes-Gasga, E. L. Martínez-Piñeiro, G. Rodríguez-Álvarez, G. E. Tiznado-Orozco, R. García-García and E. F. J. M. S. Brès, *Mater. Sci. Eng., C*, 2013, **33**, 4568–4574.
41 L. Zhang, X. Liang, J. Chen, Z. Kang, J. Ye and D. J. C. I. Xie, *Ceram. Int.*, 2024, 33153–33163.
42 C. I. Codrea, D. Lincu, I. Atkinson, D. C. Culita, A.-M. Croitoru, G. Dolete, R. Trusca, B. S. Vasile, M. S. Stan and D. J. M. Ficai, *Materials*, 2024, **17**, 1472.
43 M. Iafisco, L. Degli Esposti, G. B. Ramírez-Rodríguez, F. Carella, J. Gómez-Morales, A. C. Ionescu, E. Brambilla, A. Tampieri and J. M. Delgado-López, *Sci. Rep.*, 2018, **8**, 17016.
44 L. He, Y. Hao, L. Zhen, H. Liu, M. Shao, X. Xu, K. Liang, Y. Gao, H. Yuan, J. Li, J. Li, L. Cheng and C. van Loveren, *J. Struct. Biol.*, 2019, **207**, 115–122.
45 S. J. G. Vimalraj, *Gene*, 2020, **754**, 144855.
46 A. K. Gaharwar, S. M. Mihaila, A. Swami, A. Patel, S. Sant, R. L. Reis, A. P. Marques, M. E. Gomes and A. J. A. M. Khademhosseini, *Adv. Mater.*, 2013, **25**, 3329–3336.
47 L. Zheng, Y. Liu, L. Jiang, X. Wang, Y. Chen, L. Li, M. Song, H. Zhang, Y. S. Zhang and X. Zhang, *Acta Biomater.*, 2023, **156**, 37–48.
48 Y. Pang, C. Fu, D. Zhang, M. Li, X. Zhou, Y. Gao, K. Lin, B. Hu, K. Zhang and Q. J. A. F. M. Cai, *Adv. Funct. Mater.*, 2024, 2403233.
49 M. Li, X. Zheng, Z. Dong, Y. Zhang, W. Wu, X. Chen, C. Ding, J. Yang, J. Luo and J. Li, *Nano Res.*, 2023, **16**, 7269–7279.
50 G. J. B. a Bulaj, *Biotechnol. Adv.*, 2005, **23**, 87–92.
51 S. Tang, B. M. Richardson and K. S. Anseth, *Prog. Mater. Sci.*, 2021, **120**, 100738.
52 M. Rizwan, A. E. G. Baker and M. S. Shoichet, *Adv. Healthcare Mater.*, 2021, **10**, 2100234.
53 P. Chakma and D. Konkolewicz, *Angew. Chem., Int. Ed.*, 2019, **58**, 9682–9695.
54 Y. Liu, F. Tao, S. Miao and P. Yang, *Acc. Chem. Res.*, 2021, **54**, 3016–3027.
55 C. Fu, Z. Wang, X. Zhou, B. Hu, C. Li and P. Yang, *Chem. Soc. Rev.*, 2024, **53**, 1514–1551.
56 Y. Liu, S. Miao, H. Ren, L. Tian, J. Zhao and P. Yang, *Nat. Protoc.*, 2024, **19**, 539–564.
57 S. Lepikko, Y. M. Jaques, M. Junaid, M. Backholm, J. Lahtinen, J. Julin, V. Jokinen, T. Sajavaara, M. Sammalkorpi, A. S. Foster and R. H. A. Ras, *Nat. Chem.*, 2024, **16**, 506–513.
58 J. Yang, G. Yuan and Z. Chen, *Front. Physiol.*, 2016, **7**, 1–8.
59 H. Bakhtiar, A. Mazidi, S. Mohammadi-Asl, S. Hasannia, M. R. Ellini, M. Pezeshki-Modaress, S. N. Ostad, K. Galler, A. Azarpazhooh and A. Kishen, *J Endod.*, 2020, **46**, 57–64.
60 W. Li, M. Mao, N. Hu, J. Wang, J. Huang, W. Zhang and S. J. C. E. J. Gu, *Chem. Eng. J.*, 2021, **417**, 129299.
61 R. Shao, Y. Dong, S. Zhang, X. Wu, X. Huang, B. Sun, B. Zeng, F. Xu and W. J. B. J. Liang, *Biotechnol. J.*, 2022, **17**, 2100074.